

## Electronic Supplementary Information

### MOF-Based Colorimetric Sensor for Rapid and Visual Readout of Trace Acetylene

Jieying Hu,<sup>#a</sup> Song Chen,<sup>#a</sup> Zhiqing Liu,<sup>a</sup> Jian-Rong Li,<sup>a</sup> Jia-Hong Huang,<sup>a</sup> Zhixin Jiang,<sup>a</sup> Weihui Ou,<sup>\*a</sup> Wei-Ming Liao,<sup>a</sup> Jian Lu<sup>b</sup> and Jun He<sup>\*a</sup>

<sup>a</sup> School of Chemical Engineering and Light Industry, Guangdong University of Technology, Guangzhou, Guangdong 510006, P. R. China.

<sup>b</sup> Hong Kong Branch of National Precious Metals Material Engineering Research Centre, Department of Material Science and Engineering, City University of Hong Kong, Hong Kong 999077, China.

# These authors contributed equally to this work.

\* Corresponding author: junhe@gdut.edu.cn; weihuiou@gdut.edu.cn.

## Table of Contents

<b>Experimental details</b> .....	4
<b>Scheme S1.</b> The synthetic scheme of H <sub>2</sub> L.....	6
<b>Fig. S1.</b> Solution <sup>1</sup> H NMR spectrum of 2',5'-dimethylthio-[1,1':4',1''-terphenyl]-4,4''-dimethyl ester (Me <sub>2</sub> L) (CDCl <sub>3</sub> , 400 MHz). ....	7
<b>Fig. S2.</b> Solution <sup>13</sup> C NMR spectrum of 2',5'-dimethylthio-[1,1':4',1''-terphenyl]-4,4''-dimethyl ester (Me <sub>2</sub> L) (CDCl <sub>3</sub> , 101 MHz). ....	7
<b>Fig. S3.</b> Solution <sup>1</sup> H NMR spectrum of 2',5'-dimethylthio-[1,1':4',1''-terphenyl]-4,4''-dicarboxylic acid (H <sub>2</sub> L) (DMSO- <i>d</i> <sub>6</sub> , 400 MHz). ....	8
<b>Fig. S4.</b> Solution <sup>13</sup> C NMR spectrum of 2',5'-dimethylthio-[1,1':4',1''-terphenyl]-4,4''-dicarboxylic acid (H <sub>2</sub> L) (DMSO- <i>d</i> <sub>6</sub> , 101 MHz).....	9
<b>Fig. S5.</b> A solution <sup>1</sup> H NMR spectrum of an activated sample of <b>UiO-68-SMe</b> (5.0 mg) dissolved (dissolution facilitated by with ultrasonic vibration) in HF aqueous solution (40 wt%)/DMSO- <i>d</i> <sub>6</sub> (0.02 mL/0.45 mL). ....	10
<b>Fig. S6.</b> FT-IR spectra for (a) H <sub>2</sub> L, (b) as-made and (c) activated <b>UiO-68-SMe</b> .....	11
<b>Fig. S7.</b> Thermogravimetric analysis (TGA) plot of <b>UiO-68-SMe</b> (N <sub>2</sub> atmosphere, heating rate: 10 °C/min). ....	11
<b>Fig. S8.</b> Structures of the octahedral (a) and tetrahedral (b) cages in <b>UiO-68-SMe</b> .....	12
<b>Fig. S9.</b> Emission spectra of H <sub>2</sub> L and <b>UiO-68-SMe</b> (λ <sub>ex</sub> =370 nm). ....	12
<b>Fig. S10.</b> Emission spectra of <b>UiO-68-SMe</b> and <b>UiO-68-SMe-Pt</b> (λ <sub>ex</sub> =370 nm) .....	13
<b>Fig. S11.</b> Schematic diagrams of <b>UiO-68-SMe-Pt</b> (simplified as an octahedron-like unit) showing the proposed interaction of Pt...S and Pt .....	13
<b>Fig. S12.</b> High-resolution Pt 4f XPS spectrum of <b>UiO-68-SMe-Pt</b> .....	14
<b>Fig. S13.</b> SEM image of <b>UiO-68-SMe-Pt</b> crystals. ....	14
<b>Fig. S14.</b> (a) N <sub>2</sub> sorption isotherm at 77 K and (b) BET plot for an activated <b>UiO-68-SMe</b> . ....	14
<b>Fig.S15.</b> Pore width distribution of <b>UiO-68-SMe</b> .....	15
<b>Fig. S16.</b> (a) N <sub>2</sub> sorption isotherm at 77 K and (b) BET plot for <b>UiO-68-SMe-Pt</b> .....	15
<b>Fig. S17.</b> Photographs of <b>UiO-68-SMe-Pt</b> crystals immersed in the saturated aqueous solutions of C <sub>2</sub> H <sub>2</sub> for 15 min at varying temperature.....	16
<b>Fig. S18.</b> Photographs of <b>UiO-68-SMe-Pt</b> crystals after immersed in the aqueous solutions of various gas .....	16
<b>Fig. S19.</b> Photographs of <b>UiO-68-SMe-Pt</b> crystals after immersion in the aqueous solution of dual-component gas.....	16
<b>Fig. S20.</b> Photographs of <b>UiO-68-SMe-Pt</b> crystals immersed in the aqueous solutions of varying C <sub>2</sub> H <sub>2</sub> concentration at 70°C for 15 min. ....	16
<b>Fig. S21.</b> UV-vis-NIR absorption spectra of ligand, <b>UiO-68-SMe</b> , PtCl <sub>2</sub> and <b>UiO-68-SMe-Pt</b> .....	17
<b>Fig. S22.</b> Tauc plots and bang gaps of <b>UiO-68-SMe-Pt</b> before and after exposed to C <sub>2</sub> H <sub>2</sub> gas for 15 s, 5 min, 3 h and longer time at room temperature, respectively. ....	17
<b>Fig. S23.</b> Photographs of the set-up for <i>in situ</i> Raman measurement .....	18
<b>Fig. S24.</b> <i>In situ</i> Raman spectra of <b>UiO-68-SMe-Pt</b> exposed to C <sub>2</sub> H <sub>2</sub> gas.....	18
<b>Fig. S25.</b> Raman spectra of <b>UiO-68-SMe-Pt</b> crystals before and after immersed in the various media saturated with C <sub>2</sub> H <sub>2</sub> gas at 70°C for 15 min.....	19

<b>Fig. S26.</b> The Raman spectra of <b>UiO-68-SMe-Pt</b> crystals immersed in the aqueous solutions of varying $C_2H_2$ concentration. ....	<b>19</b>
<b>Fig. S27.</b> Photographs of <b>UiO-68-SMe</b> (a) and <b>UiO-68-SMe-Pt</b> (b) crystals before and after exposed in $C_2H_2$ for 30 min or immersion in the aqueous solution of $C_2H_2$ at $70^\circ C$ for 15 min. ....	<b>19</b>
<b>Fig. S28.</b> Raman spectra of <b>UiO-68-SMe</b> crystals before and after exposed in $C_2H_2$ for 30 min or immersed in the aqueous solution of $C_2H_2$ at $70^\circ C$ for 15 min. ....	<b>20</b>
<b>Fig. S29.</b> High-resolution Pt 4f XPS spectrum of <b>UiO-68-SMe-Pt</b> after exposed to $C_2H_2$ . ....	<b>20</b>
<b>Fig. S30.</b> PXRD patterns of <b>UiO-68-SMe-Pt</b> before and after exposed in $C_2H_2$ for 30 min or immersed in various saturated solution of $C_2H_2$ at $70^\circ C$ for 15 min. ....	<b>21</b>
<b>Fig. S31.</b> Photographs for the crystals of $Pt(CH_3CN)_2Cl_2$ before and after immersed in DI water which was pre-bubbled with $C_2H_2$ for 3 hours. ....	<b>21</b>
<b>Fig. S32.</b> Pore width distribution of <b>UiO-68-SMe-Pt</b> after exposure to $C_2H_2$ crystals for 30 min. ....	<b>21</b>
<b>Fig. S33.</b> Infrared spectra of <b>UiO-68-SMe-Pt</b> crystals before and after immersed in the various media saturated with $C_2H_2$ gas at $70^\circ C$ for 15 min. ....	<b>22</b>
<b>Fig. S34.</b> Photographs for the crystals of <b>UiO-68-SMe-Pt</b> after immersed in the transformer oil with different $C_2H_2$ concentration. ....	<b>22</b>
<b>Table S1.</b> Crystallographic refinement parameters and results of <b>UiO-68-SMe</b> . ....	<b>23</b>
<b>References</b> .....	<b>24</b>

## Experimental details

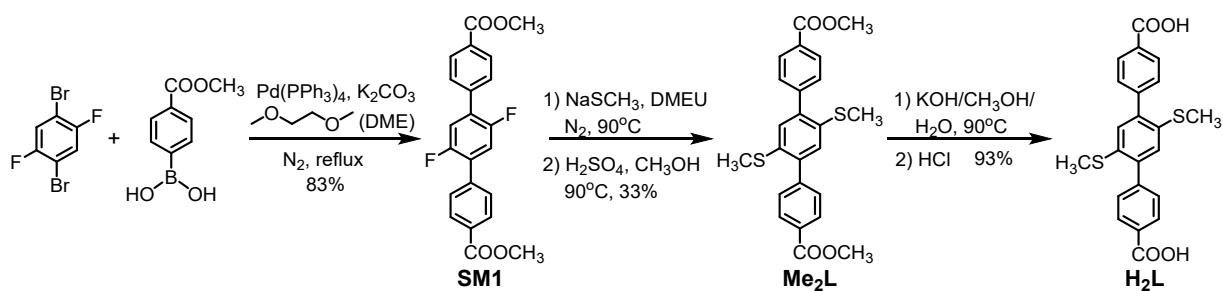
### General procedure.

All the starting materials, reagents, and solvents were purchased from commercial sources (J&K, Zhengzhou Alfa and MACKLIN) and used without additional purification. Solution  $^1\text{H}$  NMR and  $^{13}\text{C}$  NMR spectra were recorded on a 400 MHz Bruker superconducting magnet high-field NMR spectrometer at room temperature, with tetramethylsilane (TMS) as the internal standard. Chemical shifts ( $\delta$ ) are expressed in ppm relative to the residual solvent (*e.g.*, chloroform  $^1\text{H}$ : 7.26 ppm,  $^{13}\text{C}$ : 77.0 ppm) reference. Coupling constants are expressed in hertz (Hz). Solid state  $^{13}\text{C}$  NMR measurements were carried out using a Bruker Avance IIIITM HD 600 MHz spectrometer. Elemental analysis was obtained with a Elementar Vario EL cube CHNS elemental analyser. Powder X-ray diffraction (PXRD) patterns were collected on a Rigaku Smart lab diffractometer with Cu K $\alpha$  radiation ( $\lambda = 1.5418$  Å) at room temperature. The X-ray tube operated at a voltage of 40 kV and a current of 15 mA. FT-IR spectra (KBr pellet) in the range 400–4000  $\text{cm}^{-1}$  were recorded on a Thermo Fisher iS50R FT-IR spectrophotometer. Thermogravimetric analysis (TGA) was carried out on a Netzsch STA449F5 thermal analyser from 30°C to 900°C at a heating rate of 10 °C  $\text{min}^{-1}$  under N $_2$  atmosphere. The porosity and surface area analysis were performed using a Micromeritics ASAP2020 surface area and microporous physical adsorption analyzer. The sample was outgassed at 10 mm Hg with a 10°C/min ramp rate to 95°C and held for an hour, and then ramped to 120°C and held for 8 hours. The loading amount of the metal ions was determined by using a Thermo Fisher ICAP RQ inductively coupled plasma mass spectroscopy. The morphology of the samples was investigated using scanning electron microscopy (SEM, TESCAN, CLARA, Czech). X-ray photoelectron spectroscopic (XPS) measurements were conducted on a X-ray Photoelectron Spectroscopy System (Thermo Scientific K-Alpha). Fluorescence emission spectra were obtained with a FluoroMax-4 fluorescence photometer. Images of crystals were acquired with a Zeiss Observer Z1 Research Microscope. The Raman spectra were recorded at room temperature on a HORIBA Jobin Yvon Labram HR 800 UV Laser Raman Spectroscopy with a 632.8 nm red laser. The *in situ* Raman spectra were recorded in a portable Raman spectrometer (ACCUMAN SR-510 Pro, 785 nm). The molecular weights ( $M_w$  and  $M_n$ ) and polydispersity ( $M_w/M_n$ ) of the polymers were estimated in DMSO by using a Waters gel permeation chromatography (GPC) system. A set of mono-disperse polystyrene standards covering the molecular weight range of 103 to 107 was used for molecular weight calibration.

### Single crystal X-ray crystallography.

Single crystals of **UiO-68-SMe** were pretreated by soaking in the acetonitrile solution of PdCl $_2$  before test. Single crystal data for **UiO-68-SMe** were collected using a Bruker APEX-II CCD diffractometer with an I- $\mu$ -S micro-focus X-ray source using Mo K $\alpha$  radiation ( $\lambda = 0.71073$  Å) at 100 K. Reflections were indexed and processed, and the files were corrected for absorption using APEX3 v2018. The space group was assigned, the structure was solved by direct methods using ShelXS $^1$  and refined by full matrix least squares against  $F^2$  with all reflections using ShelXL $^2$  of Olex2 $^3$  software packages. All non-hydrogen atoms were refined with anisotropic thermal parameters, and all hydrogen atoms were included in calculated positions and refined with isotropic thermal parameters riding on those of the parent atoms. The structure shows substantial disorder of various kinds. Part of the disorder was modeled based on electron densities and known chemical identity of fragments. Excessive disorder of solvent molecules and absorbed metal salts were ignored as no indication was found in the difference

maps. Within the Zr-oxygen cluster, oxo and hydroxo ions are disordered in a 1:1 ratio over symmetry equivalent positions, with the hydroxo ions having slightly longer Zr-O bonds than the oxo ions. Electron density in hydrogen bonding distance to the half occupied hydroxo ion was refined as a water molecule, also with half occupancy. Hydrogen atoms were ignored for the water molecule. The organic linkers show multiple disorder due to a symmetry of the linkers that does not match the crystallographic site symmetry. Additional disorder is caused by tilting of the aromatic rings and by slight bending of the ligands from an ideal straight geometry. The ligands were refined as disordered over eight symmetry equivalent sites of which each two are exactly identical. The latter was done for refinement strategy reasons, to allow to constrain the aromatic rings to an ideal geometry, see below. All aromatic rings were constrained to resemble ideal hexagons with C-C bonding distances of 1.39 Angstroms. Equivalent bond distances within the ligand, if not already covered by the above constraint, were restrained to be the same within a standard deviation of 0.02 Angstrom. This involved the C-S distances, the C-C distances between rings, the 1,3 distances around the C atoms connecting the aromatic rings on both sides of the central aromatic ring, and the 1,3 C-C distances around the sulfur atoms. The latter were also restrained to be at least three Angstroms. The S-C(methyl) distances were restrained to 1.87(2) Angstroms. Non-H atoms connected to any of the aromatic rings were restrained to be in plane with the aromatic ring. The ADPs of overlapping disordered atoms were constrained to be identical. The atom pairs in question are C3 and C3B; C4 and C4B; C6 and C6B; C7, C7B, C7C and C7D; S1 and S1B; and C8 and C8B. All ligand carbon and sulfur atoms were also restrained to have similar and close to isotropic ADPs (SIMU, DELU and ISOR commands in Shelx, esds of 0.1, 0.1 and 0.02 Angstrom squared, respectively.) The structure contains solvent accessible voids of 17528 Angstrom cubed. The voids are filled solvate molecules. The largest residual electron density is however less than 1.6 electrons per cubic Angstrom. Due to the excessively disordered nature of these molecules, the content of the voids was ignored in the refinement model, and corrected instead using the SQUEEZE algorithm as implemented in PLATON.<sup>4</sup> The algorithm yielded 6360 electrons that were corrected for in the major void. See the Squeeze report appended to the cif file for details. Four low angle reflections were affected by the beam stop and were omitted from the refinement. The reflections in question are 0 2 2, 2 2 2, 0 0 2, and 1 1 1. Details of refinement results are listed in **Table S1**. Complete crystallographic data for **UiO-68-SMe**, in CIF format, have been deposited with the Cambridge Crystallographic Data Centre as CCDC number 2234821. These data can be obtained free of charge from The Cambridge Crystallographic Data Centre *via* [www.ccdc.cam.ac.uk/data\\_request/cif](http://www.ccdc.cam.ac.uk/data_request/cif).



**Scheme S1.** The synthetic scheme of  $H_2L$ .

**Synthesis of 2',5'-difluorine-[1,1':4',1''-terphenyl]-4,4''-dimethyl ester (SM1).** Compound **SM1** was prepared according to a recent work.<sup>5</sup> A two-neck round-bottomed flask (250 mL) was charged with a magnetic stirring bar, 1,4-dibromo-2,5-difluoro-benzene (1.17 g, 4.30 mmol), 4-methoxycarbonylphenylboronic acid (1.86 g, 10.33 mmol), potassium carbonate (3.57 g, 25.83 mmol), and tetrakis (triphenylphosphine) palladium (0.12 g, 0.10 mmol). Then, the flask was evacuated and back-filled with  $N_2$  gas for three times. Ethylene glycol dimethyl ether (DME, 70 mL) was purged by bubbling  $N_2$  gas for 15 minutes and injected into the flask *via* cannula under  $N_2$ . Afterward, the flask was connected to a condenser and the mixture was refluxed for 72 h under  $N_2$  protection. After the reaction mixture was cooled to room temperature, the solvent was removed with a rotary evaporator and the residue was re-dissolved in dichloromethane. The organic mixture was washed extensively with brine (200 mL  $\times$  3) and dried over  $Na_2SO_4$ . After removal of the solvent on a rotary evaporator, the residue was further purified by column chromatography (silica gel,  $CH_2Cl_2$  as eluent) to yield compound **SM1** as a white solid (1.17 g, 71% yield based on 1,4-dibromo-2,5-difluoro-benzene).

**Synthesis of 2',5'-dimethylthio -[1,1':4',1''-terphenyl]-4,4''-dimethyl ester ( $Me_2L$ ).** A two-neck flask (100 mL) was charged with a magnetic stirring bar, compound **SM1** (1.04 g, 2.72 mmol) and sodium methanethiolate (2.20 g, 31.39 mmol). The flask was evacuated and back-filled with  $N_2$  gas for three times. DMEU (1,3-dimethyl-2-imidazolidinone, 24 mL) was purged by bubbling  $N_2$  gas for 15 minutes and injected into the flask *via* cannula under  $N_2$ . The reaction mixture was then stirred and heated at 90°C under nitrogen protection. After two days, the reaction mixture was poured into 100 mL of distilled water, whose pH was adjusted below 2 with 10% HCl. A yellow precipitate was collected by filtration and washed extensively with distilled water. Thus-obtained resultant solid, methanol (20 mL) and  $H_2SO_4$  (2.0 mL, concentration: 95% ~ 97%) were added into a round-bottom flask and stirred at 90°C for 24 h. After cooling to room temperature, the reaction mixture was poured into 200 mL of water. The precipitate was collected by filtration and re-dissolved in dichloromethane. After removal of the solvent on a rotary evaporator, the residue was further purified by column chromatography (silica gel, 1:1 petroleum ether/ $CH_2Cl_2$  as eluent) to yield compound  $Me_2L$  as a light-yellow solid (0.394 g, 33% yield based on compound **SM1**).  $^1H$  NMR (400 MHz,  $CDCl_3$ )  $\delta$  = 8.13 (d,  $J$  = 8.4 Hz, 2H), 7.55 (d,  $J$  = 8.4 Hz, 2H), 7.15 (s, 1H), 3.95 (s, 3H), 2.34 (s, 3H).  $^{13}C$  NMR (101 MHz,  $CDCl_3$ )  $\delta$  = 166.81, 144.49, 140.28, 133.73, 129.53, 129.48, 129.36, 127.56, 52.17, 16.40.

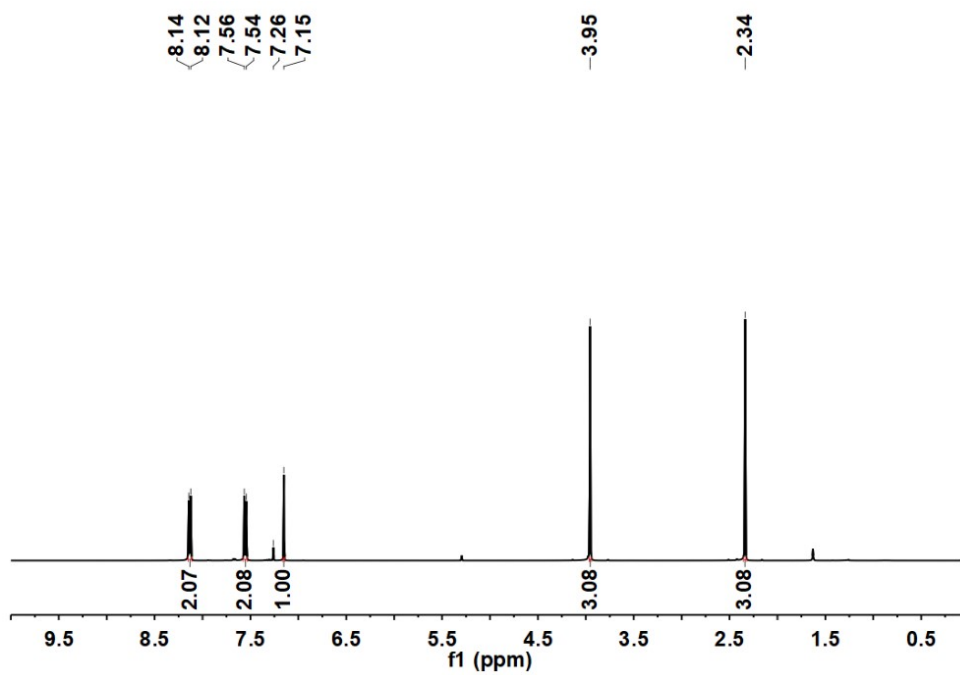


**Fig. S1.** Solution  $^1\text{H}$  NMR spectrum of 2',5'-dimethylthio-[1,1':4',1''-terphenyl]-4,4''-dimethyl ester ( $\text{Me}_2\text{L}$ ) ( $\text{CDCl}_3$ , 400 MHz).

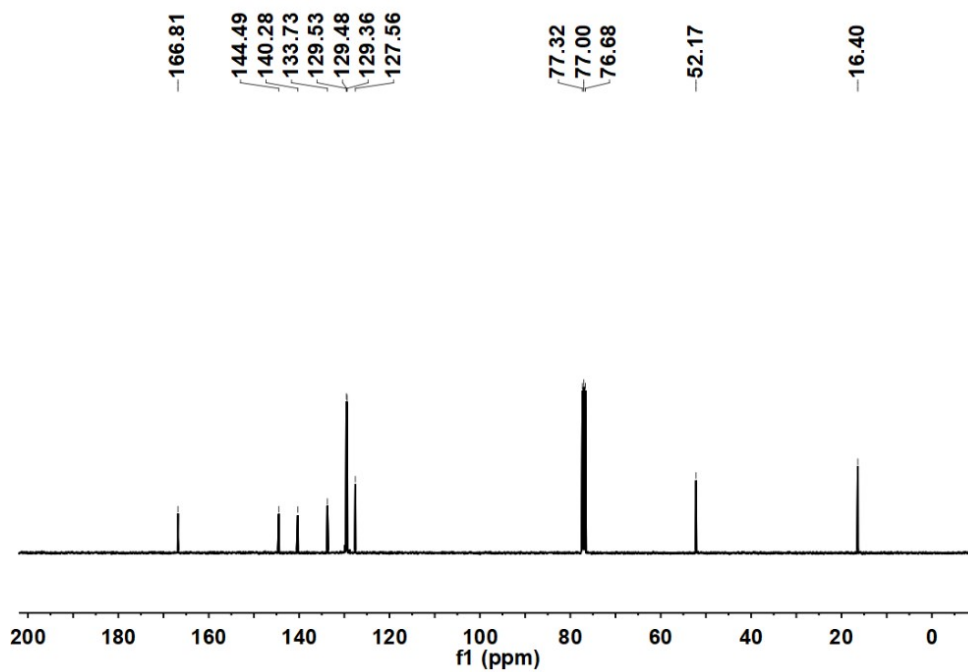


**Fig. S2.** Solution  $^{13}\text{C}$  NMR spectrum of 2',5'-dimethylthio-[1,1':4',1''-terphenyl]-4,4''-dimethyl ester ( $\text{Me}_2\text{L}$ ) ( $\text{CDCl}_3$ , 101 MHz).

**Synthesis of 2',5'-dimethylthio-[1,1':4',1''-terphenyl]-4,4''-dicarboxylic acid (H<sub>2</sub>L).** Compound Me<sub>2</sub>L (393.8 mg, 0.898 mmol) and an aqueous solution mixture of KOH (7 M, 30 mL in CH<sub>3</sub>OH/H<sub>2</sub>O, volume ratio of 1/1) were added to a round-bottom flask charged with a magnetic stirring bar. The mixture was stirred at 90°C for 24 h. After cooling to room temperature, the reaction mixture was poured into 150 mL of water, whose pH was adjusted below 2 with HCl (concentration: ~37wt%). A yellow precipitate was collected by filtration and washed extensively with distilled water. Thus-obtained light-yellow solid was termed H<sub>2</sub>L (342.6 mg, 93% yield based on Me<sub>2</sub>L). <sup>1</sup>H NMR (400 MHz, DMSO-*d*<sub>6</sub>) δ = 8.03 (d, *J* = 8.1 Hz, 2H), 7.59 (d, *J* = 8.1 Hz, 2H), 7.18 (s, 1H), 2.38 (s, 3H). <sup>13</sup>C NMR (101 MHz, DMSO-*d*<sub>6</sub>) δ = 167.57, 144.22, 139.89, 133.67, 130.63, 129.90, 129.69, 127.30, 15.83.

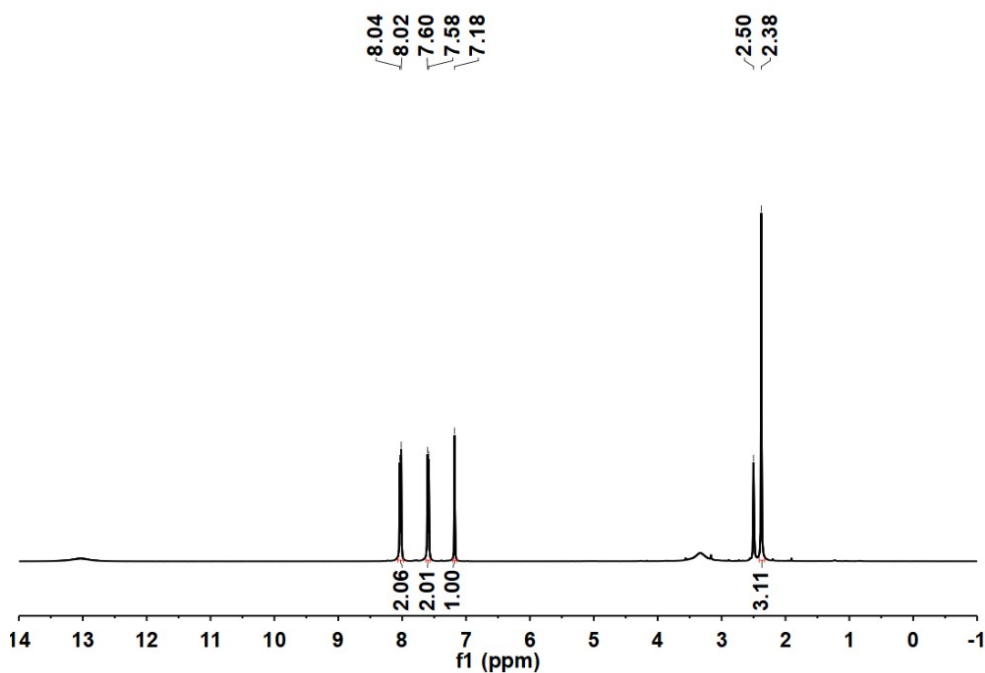


**Fig. S3.** Solution <sup>1</sup>H NMR spectrum of 2',5'-dimethylthio-[1,1':4',1''-terphenyl]-4,4''-dicarboxylic acid (H<sub>2</sub>L) (DMSO-*d*<sub>6</sub>, 400 MHz).



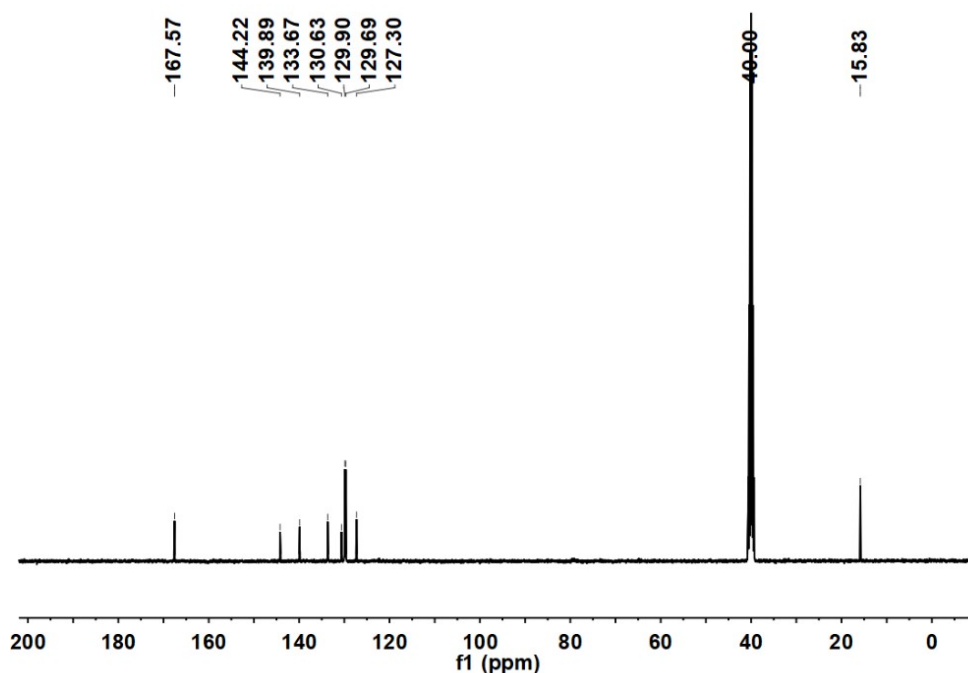


**Fig. S4.** Solution  $^{13}\text{C}$  NMR spectrum of 2',5'-dimethylthio-[1,1':4',1''-terphenyl]-4,4''-dicarboxylic acid ( $\text{H}_2\text{L}$ ) ( $\text{DMSO-}d_6$ , 101 MHz).

**Crystallization and activation of UiO-68-SMe.**  $\text{ZrCl}_4$  (8 mg, 0.034 mmol), ligand  $\text{H}_2\text{L}$  (10 mg, 0.024 mmol) and benzoic acid (80 mg, 0.655 mmol) were ultrasonically dissolved in DMF (1.0 mL) and then flame-sealed in a Pyrex glass tube (soda lime, 10 mm OD, 8 mm ID). The tube was then heated at  $130^\circ\text{C}$  in an oven for 72 hours and cooled to room temperature naturally. Octahedron shape colorless single crystals suitable for single-crystal X-ray diffraction obtained were filtered, washed by DMF (5 mL) and acetonitrile (5 mL) and evacuated at room temperature to yield the as-made sample of **UiO-68-SMe** (yield: 8.0 mg, 57% based on  $\text{H}_2\text{L}$ ). The as-made crystals of **UiO-68-SMe** were soaked in acetonitrile at room temperature for solvent exchange (the supernatant was replaced by fresh acetonitrile every 4 hours,  $5 \times 3$  mL). Then the crystals were evacuated at  $80^\circ\text{C}$  for 2 hours to obtain the activated sample of **UiO-68-SMe**. Elemental analysis found C (48.46%), H (3.487%) N (0.33%) and S (10.85%) for activated **UiO-68-SMe**, which fits the formula of  $\text{Zr}_6\text{O}_4(\text{OH})_4(\text{L})_{5.3}(\text{C}_7\text{H}_5\text{O}_2)_{1.4}(\text{H}_2\text{O})_5$  (MW: 3103.98).

**Preparation of UiO-68-SMe-Pt.** A 25 mL two-neck flask was loaded with  $\text{PtCl}_2$  (30 mg) and acetonitrile (5 mL), which was bubbled with nitrogen for 15 min and heated at  $70^\circ\text{C}$  for 4 hours. The resultant solution was filtered to obtain the saturated acetonitrile solution of  $\text{Pt}(\text{CH}_3\text{CN})_2\text{Cl}_2$ . 5 mg of **UiO-68-SMe** crystals were soaked in 1.5 mL of the saturated acetonitrile solution of  $\text{Pt}(\text{CH}_3\text{CN})_2\text{Cl}_2$  at room temperature. Concomitantly, the crystals changed from colorless to light-yellow. After 24 hours, the resultant light-yellow crystals were wash with acetonitrile to obtain **UiO-68-SMe-Pt**. The crystals were stored in acetonitrile for future usage.

**Preparation of saturated aqueous solution of different gases ( $\text{H}_2$ ,  $\text{N}_2$ ,  $\text{CO}_2$ ,  $\text{C}_2\text{H}_2$ ,  $\text{C}_2\text{H}_4$  and  $\text{C}_2\text{H}_6$ ).** 20 mL of deionized water was added into a 50 mL round-bottomed flask and bubbled with different gases for 40 minutes, respectively. The resultant solution was regarded as saturated.

**Preparation of saturated solution of C<sub>2</sub>H<sub>2</sub>.** Various solution (20 mL, acetone, acetonitrile, cyclohexane and ethanol) was added into a 50 mL round-bottomed flask and bubbled with C<sub>2</sub>H<sub>2</sub> for 40 minutes, respectively. The resultant solution was regarded as saturated.

**Sensing experiment in gas phase.** 3 mg of UiO-68-SMe-Pt crystals were added into a 25 mL round-bottomed flask and purged with different gases (H<sub>2</sub>, N<sub>2</sub>, CO<sub>2</sub>, C<sub>2</sub>H<sub>4</sub> and C<sub>2</sub>H<sub>6</sub>) at room temperature.

**Sensing experiment in the solution phase.** 3 mg of UiO-68-SMe-Pt crystals were added into a 10 mL glass vial and immersed in varying solutions in an oven at 70°C, which were pre-purged with different gases (H<sub>2</sub>, N<sub>2</sub>, CO<sub>2</sub>, C<sub>2</sub>H<sub>2</sub>, C<sub>2</sub>H<sub>4</sub> and C<sub>2</sub>H<sub>6</sub>) for 15 minutes.

**Gel permeation chromatography.** The sample (~ 25 mg) was digested in HF/DMSO (0.1 mL/5 mL) by ultrasonication until completely dissolved, and then the resultant solution was filtered by membrane (0.25 mm).

**Sample preparation for inductively coupled plasma mass spectroscopy (ICP-MS).** UiO-68-SMe-Pt (5.21 mg) was added into a 10 mL glass vial, following by the addition of conc. H<sub>2</sub>SO<sub>4</sub> (concentration: 97~99wt%), conc. HCl (concentration: 37wt%) and conc. HNO<sub>3</sub> (concentration: ≥65%). The above mixture was stirred for 12 hours at 90°C to obtain a yellow solution. After cooling to room temperature, the resulting mixture was diluted with DI water to ~100.0 mL and the aqueous solution was filtered by membrane (0.22 mm) and further diluted by 100 times, and then immediately used for ICP-MS tests. ICP-MS results show the weight concentrations of Zr and Pt are respectively 78.640 mg/L and 25.422 mg/L, indicating that the atomic ratio of Zr and Pt equals to 6: 0.9.

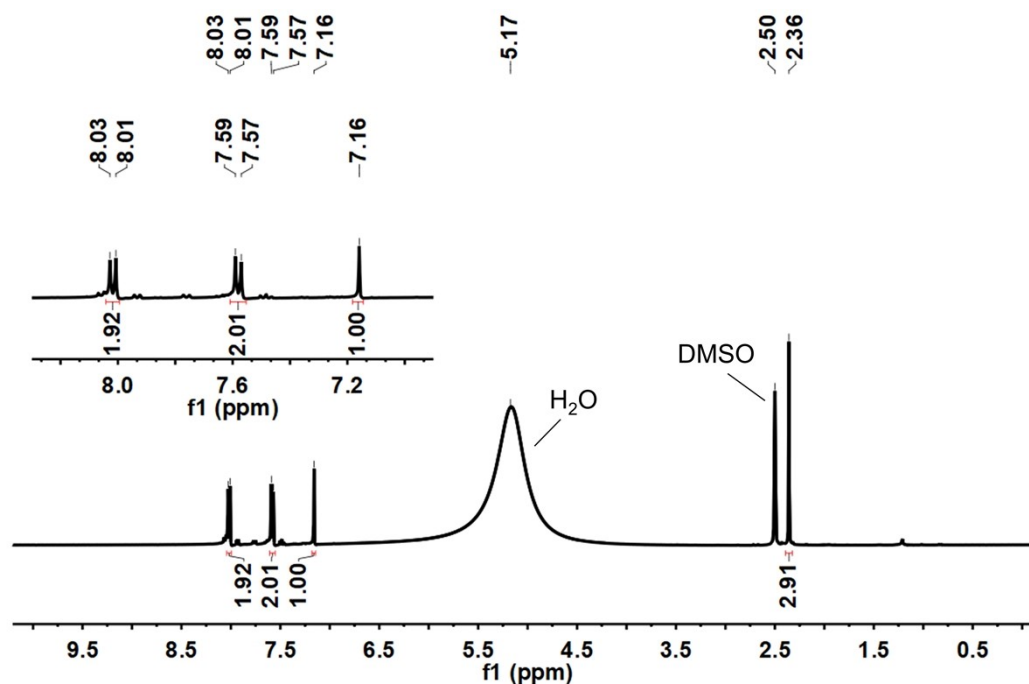


**Fig. S5.** A solution <sup>1</sup>H NMR spectrum of an activated sample of UiO-68-SMe (5.0 mg) dissolved with ultrasonication in a solvent mixture of HF aqueous solution (40 wt%) and DMSO-*d*<sub>6</sub>.

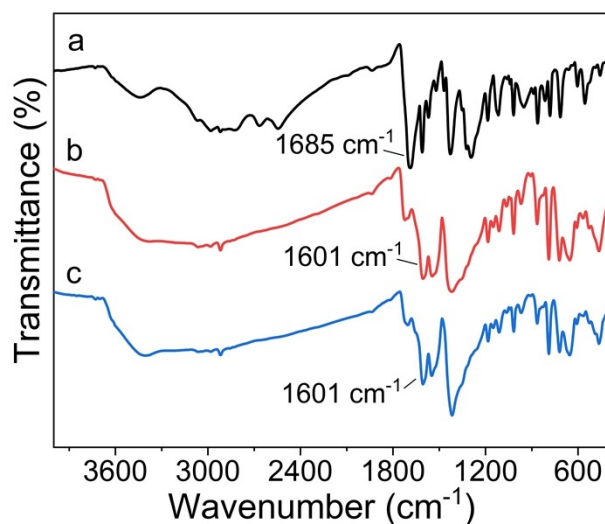


**Fig. S6.** FT-IR spectra of (a)  $\text{H}_2\text{L}$ , (b) as-made and (c) activated **UiO-68-SMe** crystals.

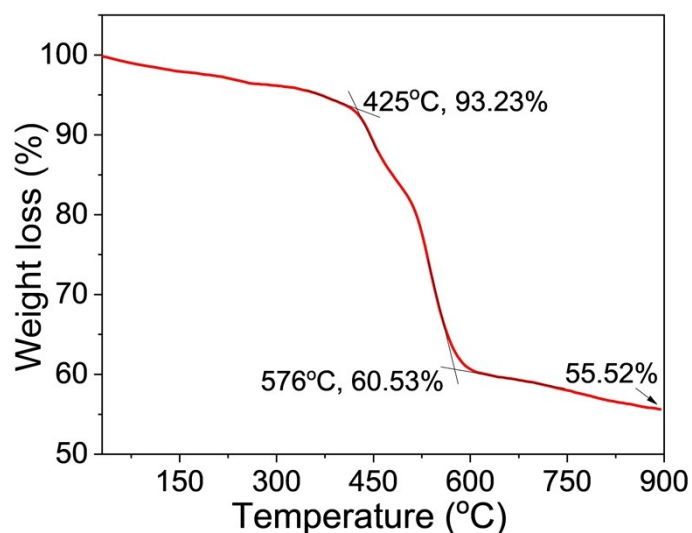


**Fig. S7.** Thermogravimetric analysis (TGA) plot of **UiO-68-SMe** ( $\text{N}_2$  atmosphere, heating rate:  $10\text{ }^\circ\text{C}/\text{min}$ ).

**UiO-68-SMe:** The weight loss ( $100\% - 60.53\% = 39.47\%$ ) up to  $576\text{ }^\circ\text{C}$  corresponds to the departure of the water molecules (total number: 5),  $\text{C}_6\text{H}_5\text{COO}^-$  (total number: 1.4),  $-\text{SCH}_3$  (total number: 10.6] and  $\text{COO}^-$  (total number: 10.6), from the formula (fresh sample with lower water molecule number):  $\text{Zr}_6\text{O}_4(\text{OH})_4(\text{L})_{5.3}(\text{C}_7\text{H}_5\text{O}_2)_{1.4}(\text{H}_2\text{O})_5$  (mw 3103.98):  $5\text{H}_2\text{O} + 1.4\text{C}_7\text{H}_5\text{O}_2^- + 10.6\text{SCH}_3 + 10.6\text{COO}^- = 1225.33$ ;  $1225.33/3103.98 = 39.48\%$ . The substantial residual weight at (55.52%) at  $900^\circ\text{C}$  suggests the presence of carbon/Zr-based solid.

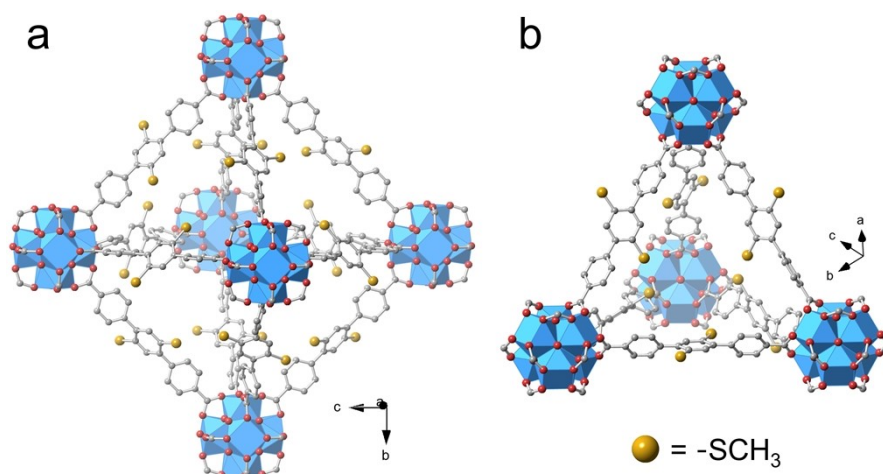


**Fig. S8.** Structures of the octahedral (a) and tetrahedral (b) cages in **UiO-68-SMe**. H atoms were omitted for clarity. Red spheres, O; gray, C; yellow, -SCH<sub>3</sub>; blue, Zr-based polyhedrons.

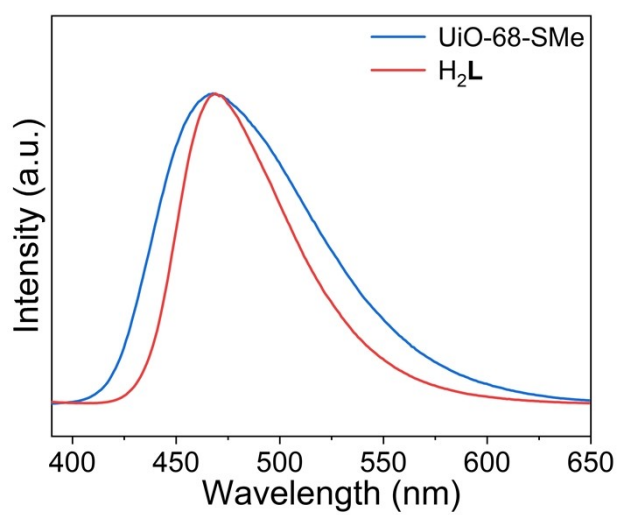


**Fig. S9.** Emission spectra of H<sub>2</sub>L and **UiO-68-SMe** ( $\lambda_{\text{ex}}=370$  nm).

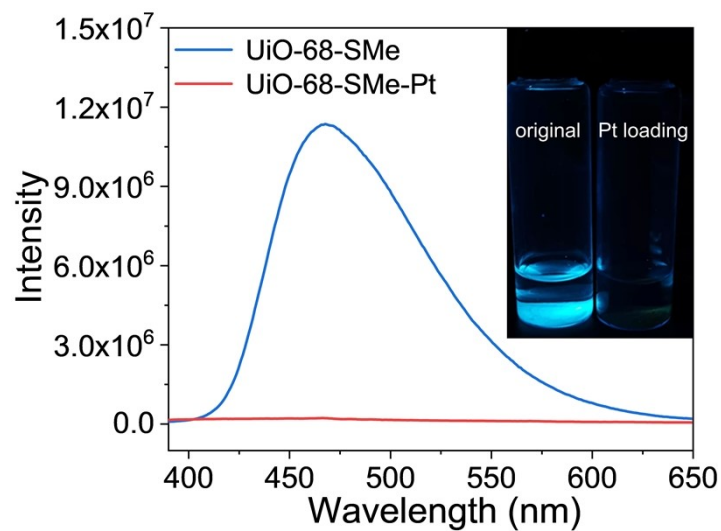


**Fig. S10.** Emission spectra of **UiO-68-SMe** and **UiO-68-SMe-Pt** ( $\lambda_{\text{ex}} = 370$  nm), with their photographs shown in the inset.

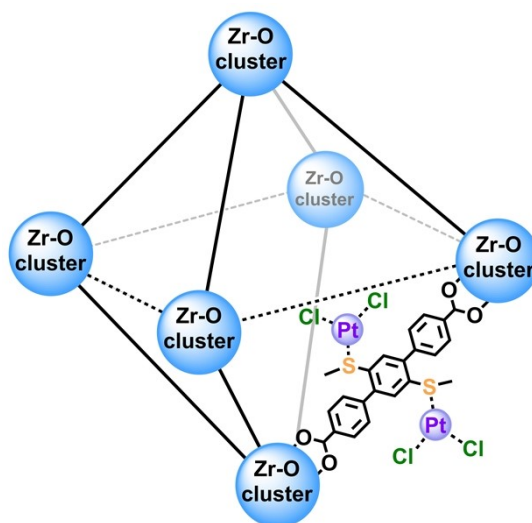


**Fig. S11.** Schematic of the proposed interaction of Pt...S and Pt...Cl in **UiO-68-SMe-Pt**.

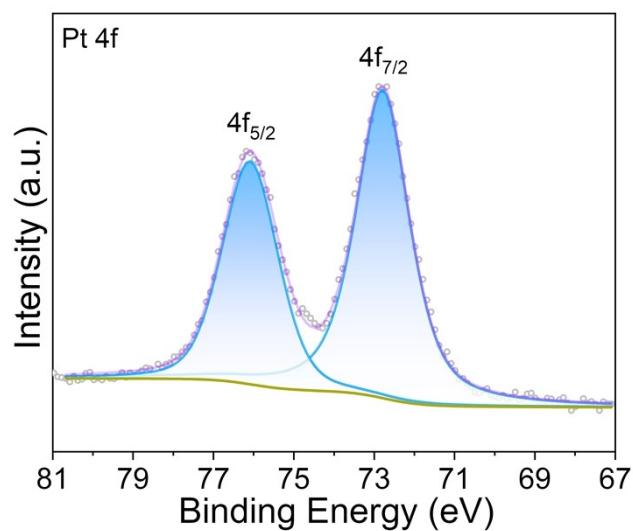


Fig. S12. High-resolution Pt 4f XPS spectrum of UiO-68-SMe-Pt.

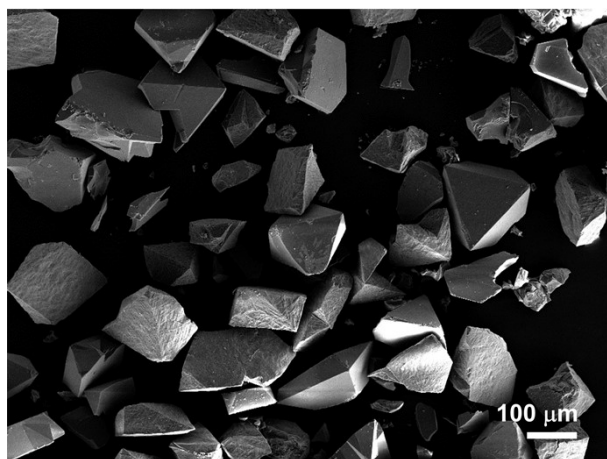


Fig. S13. SEM image of UiO-68-SMe-Pt crystals.

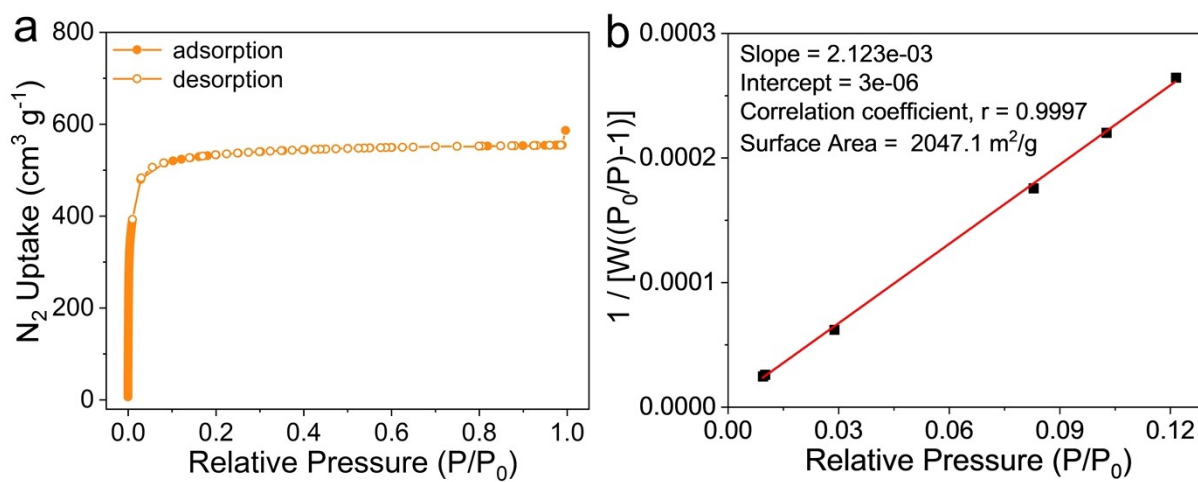


Fig. S14. (a)  $N_2$  sorption isotherm of activated UiO-68-SMe at 77 K and (b) the fitting BET plot.

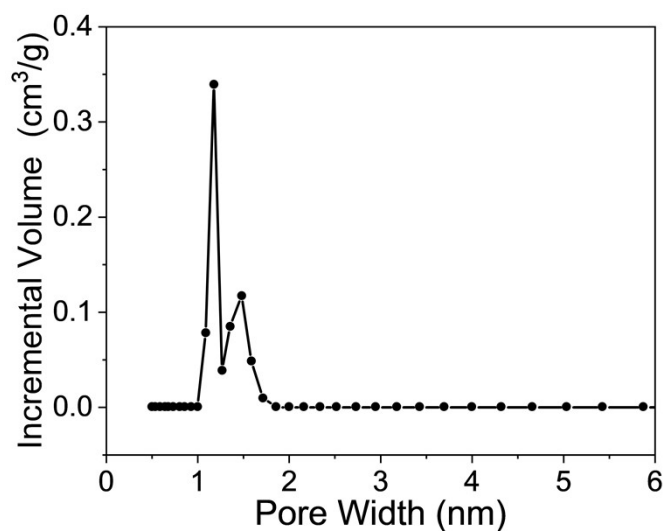


Fig. S15. Pore width distribution of UiO-68-SMe.

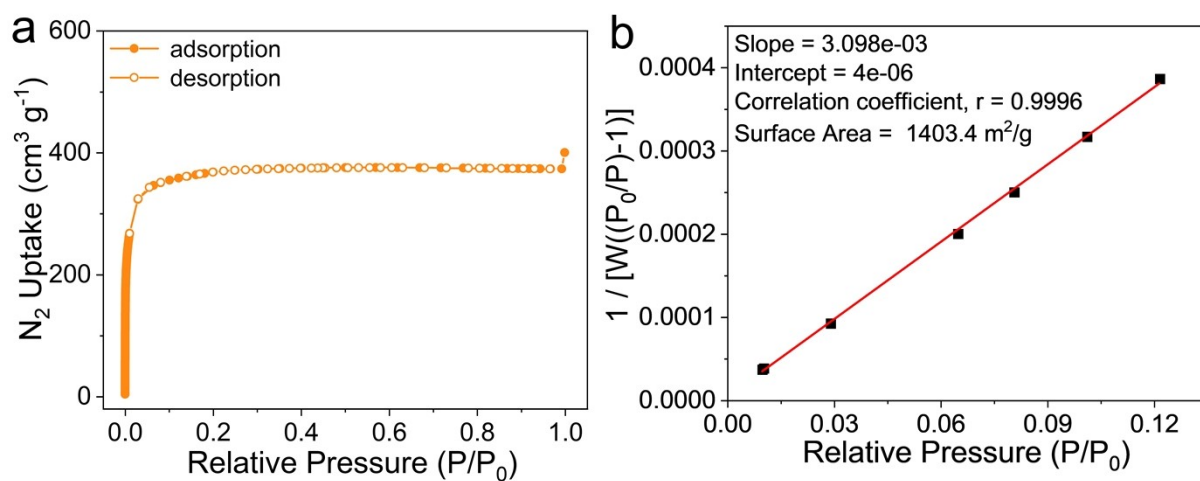
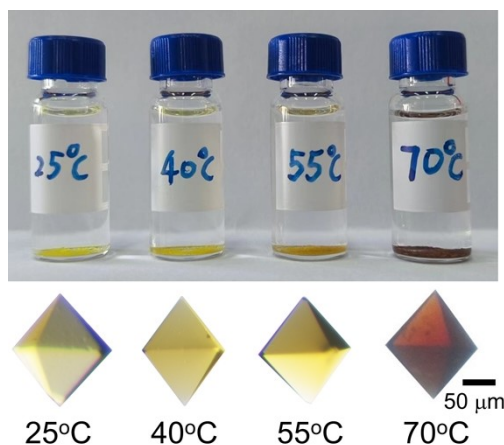
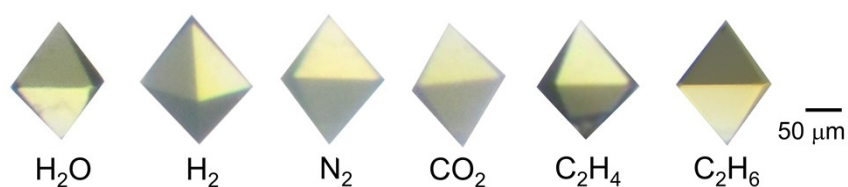


Fig. S16. (a)  $N_2$  sorption isotherm of UiO-68-SMe-Pt at 77 K and (b) the fitting BET plot.



**Fig. S17.** Photographs of **UiO-68-SMe-Pt** crystals immersed in the saturated aqueous solutions of  $C_2H_2$  for 15 min at varying temperature.



**Fig. S18.** Photographs of **UiO-68-SMe-Pt** crystals after immersed in the aqueous solutions of various gas at  $70^\circ C$  for 15 min.

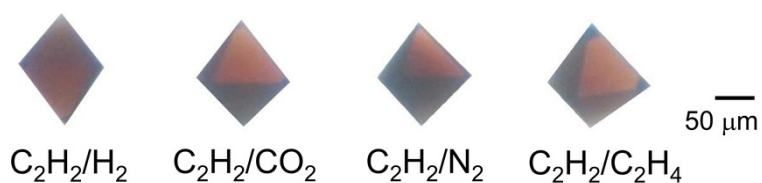


**Fig. S19.** Photographs of **UiO-68-SMe-Pt** crystals after immersion in the aqueous solution of dual-component gas at  $70^\circ C$  for 15 min.

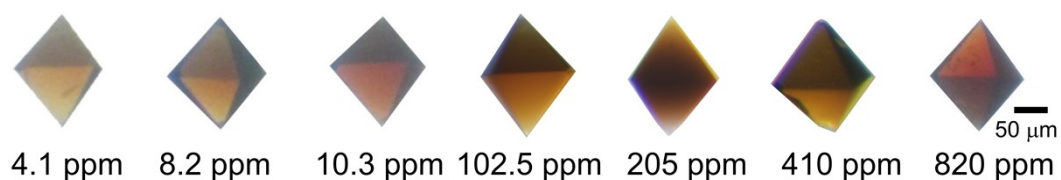


**Fig. S20.** Photographs of **UiO-68-SMe-Pt** crystals immersed in the aqueous solutions of varying  $C_2H_2$  concentration at  $70^\circ C$  for 15 min.



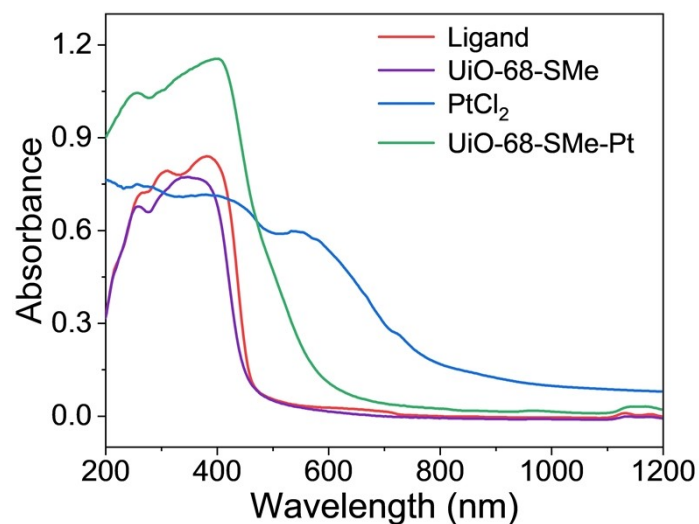


**Fig. S21.** UV-vis-NIR absorption spectra of ligand, UiO-68-SMe, PtCl<sub>2</sub> and UiO-68-SMe-Pt.

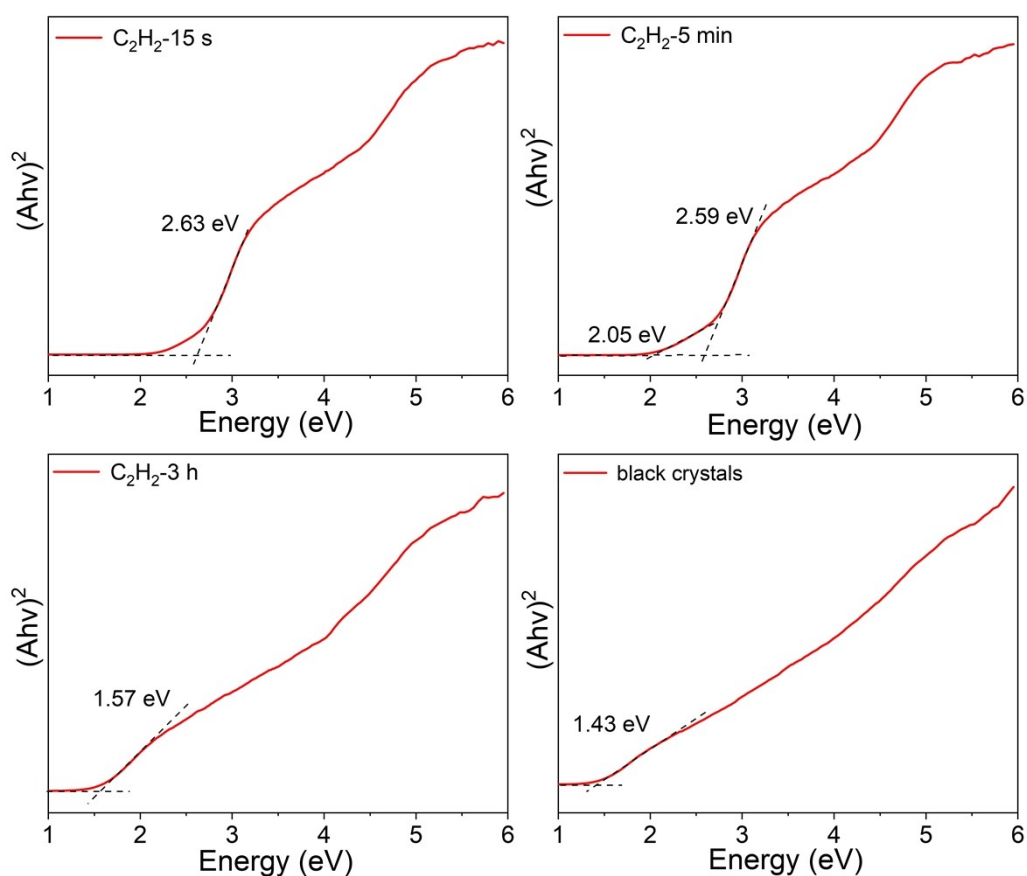


**Fig. S22.** Tauc plots and bang gaps of UiO-68-SMe-Pt before and after exposed to C<sub>2</sub>H<sub>2</sub> gas for 15 s, 5 min, 3 h and longer time at room temperature, respectively.

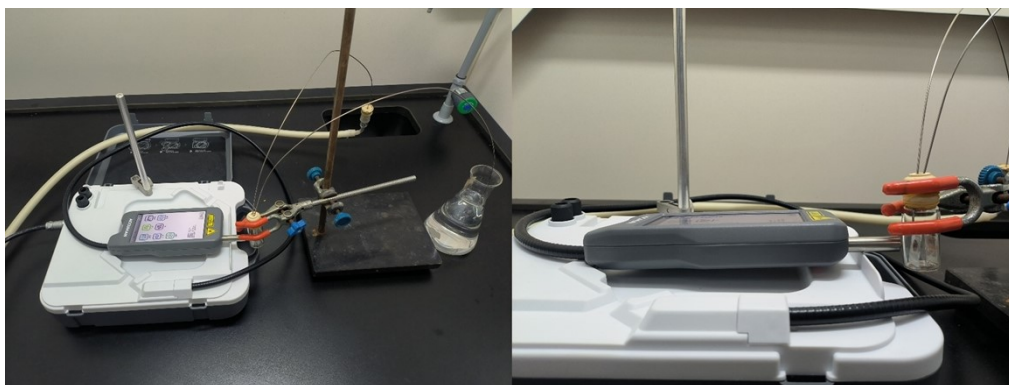


Fig. S23. Photographs of the set-up for *in situ* Raman measurement.

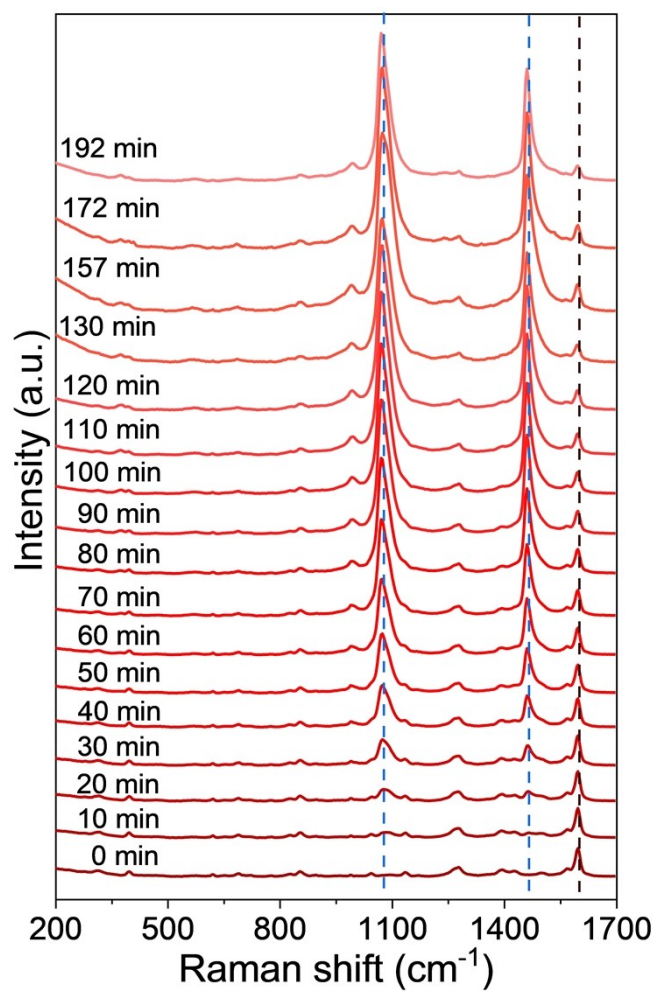
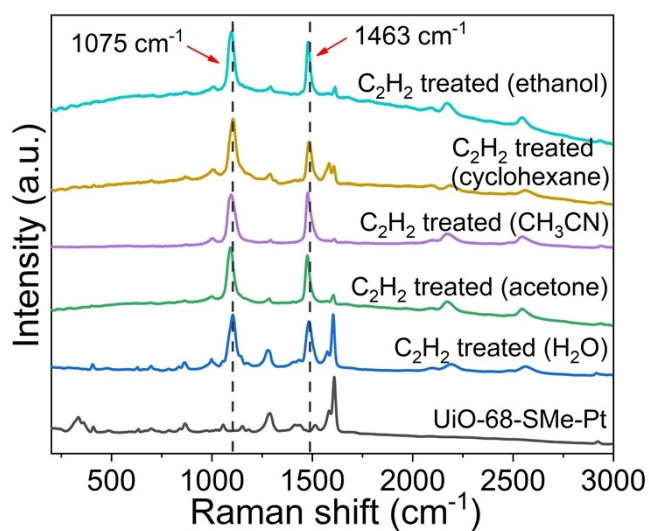
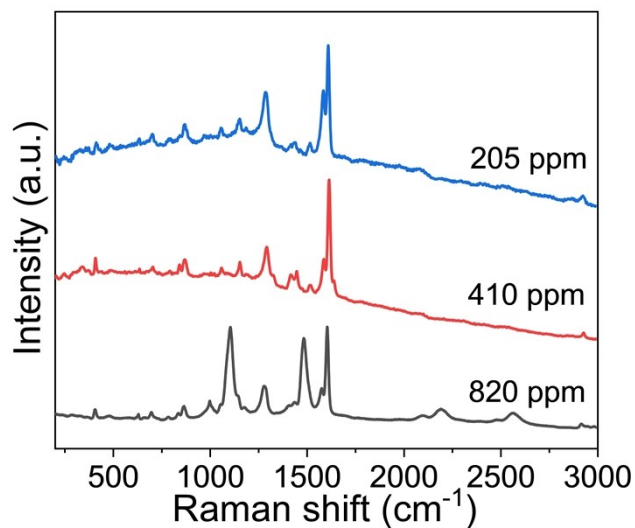


Fig. S24. *In situ* Raman spectra of UiO-68-SMe-Pt exposed to  $\text{C}_2\text{H}_2$  gas.



**Fig. S25.** Raman spectra of **UiO-68-SMe-Pt** crystals before and after immersed in the various media saturated with  $C_2H_2$  gas at  $70^\circ C$  for 15 min



**Fig. S26.** The Raman spectra of **UiO-68-SMe-Pt** crystals immersed in the aqueous solutions of varying  $C_2H_2$  concentration.

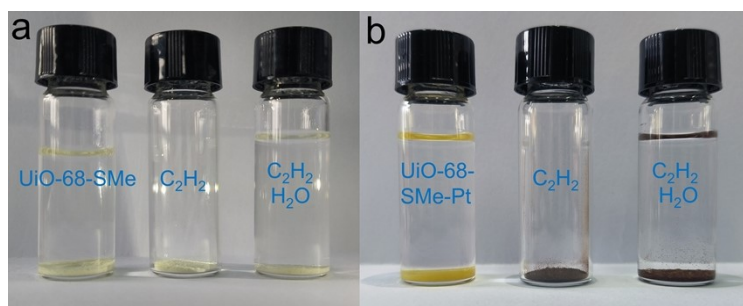


**Fig. S27.** Photographs of **UiO-68-SMe** (a) and **UiO-68-SMe-Pt** (b) crystals before and after exposed in  $C_2H_2$  for 30 min or immersion in the aqueous solution of  $C_2H_2$  at  $70^\circ C$  for 15 min.

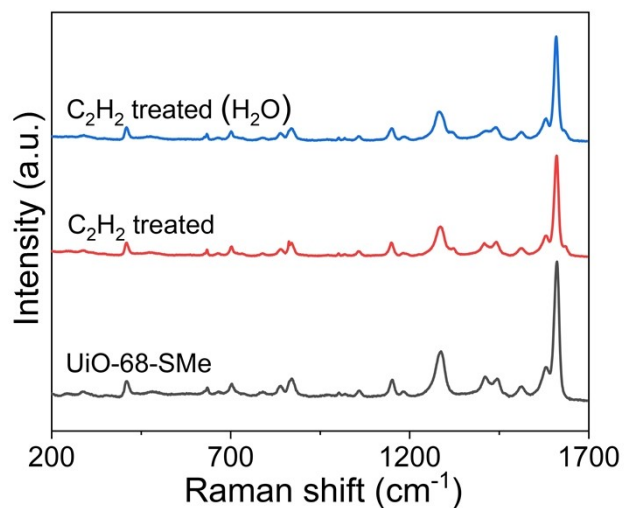


**Fig. S28.** Raman spectra of **UiO-68-SMe** crystals before and after exposed to  $C_2H_2$  for 30 min or immersed in the aqueous solution of  $C_2H_2$  at 70°C for 15 min.

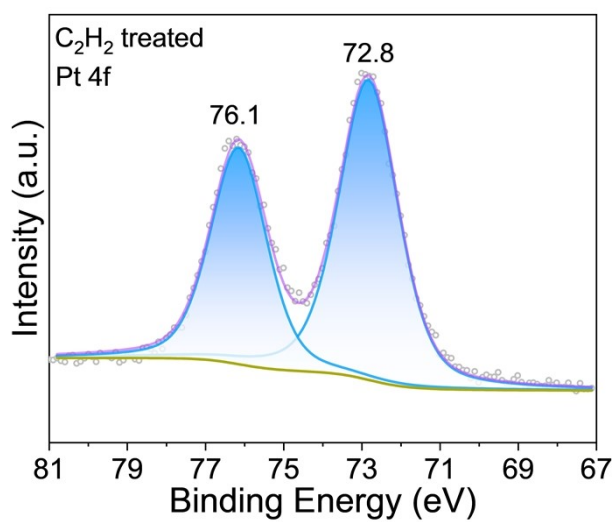


**Fig. S29.** High-resolution Pt 4f XPS spectrum of **UiO-68-SMe-Pt** after exposed to  $C_2H_2$ .

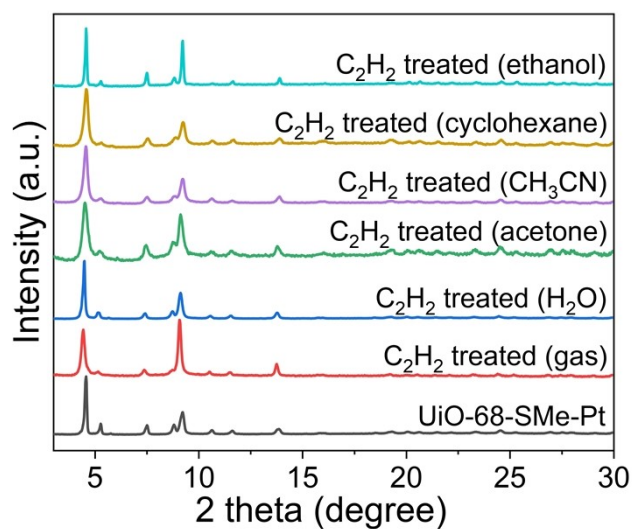


**Fig. S30.** PXRD patterns (Cu K $\alpha$ ,  $\lambda = 1.5418 \text{ \AA}$ ) of **UiO-68-SMe-Pt** before and after purged with for 30 min or exposed to C<sub>2</sub>H<sub>2</sub> in various matrices at 70°C for 15 min.

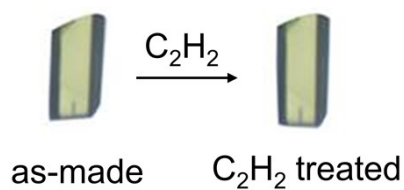


**Fig. S31.** Photographs of the Pt(CH<sub>3</sub>CN)<sub>2</sub>Cl<sub>2</sub> crystals before and after immersed in DI water which was pre-bubbled with C<sub>2</sub>H<sub>2</sub> for 3 hours.

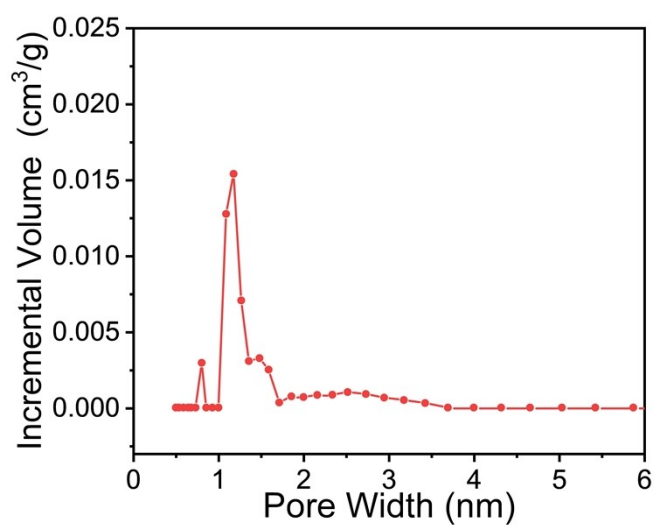


**Fig. S32.** Pore width distribution of **UiO-68-SMe-Pt** after exposure to C<sub>2</sub>H<sub>2</sub> for 30 min.

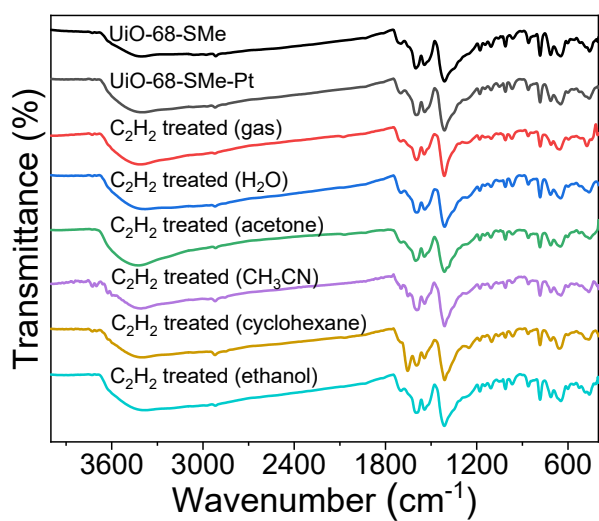


**Fig. S33.** Infrared spectra of **UiO-68-SMe-Pt** crystals before and after immersed in the various media saturated with  $\text{C}_2\text{H}_2$  gas at  $70^\circ\text{C}$  for 15 min.



**Fig. S34.** Photographs of the **UiO-68-SMe-Pt** crystals after immersed in the transformer oil with different  $\text{C}_2\text{H}_2$  concentration and varying periods.

**Table S1.** Crystallographic refinement parameters and results of UiO-68-SMe.

Compound	UiO-68-SMe
CCDC number	2234821
Empirical formula	C <sub>126</sub> H <sub>82</sub> O <sub>36</sub> S <sub>6</sub> Zr <sub>6</sub>
Formula weight	2911.59
Temperature/K	100
Crystal system	cubic
Space group	<i>Fm-3m</i> (225)
<i>a</i> /Å	32.575(2)
<i>b</i> /Å	32.575(2)
<i>c</i> /Å	32.575(2)
<i>α</i> °	90.00
<i>β</i> °	90.00
<i>γ</i> °	90.00
Volume/Å <sup>3</sup>	34568(8)
Z	4
<i>D<sub>c</sub></i> /g·cm <sup>-3</sup>	0.559
<i>μ</i> /mm <sup>-1</sup>	0.239
<i>F</i> (000)	5851.2
<i>R</i> <sub>1</sub> <sup>a</sup> ( <i>I</i> > 2σ( <i>I</i> ))	0.0833
<i>wR</i> <sub>2</sub> <sup>b</sup> (all data)	0.2680
GOF on <i>F</i> <sup>2</sup>	1.151

$$^a R_1 = \sum(|F_o| - |F_c|) / \sum|F_o|; \quad ^b wR_2 = (\sum w(F_o^2 - F_c^2)^2 / \sum w(F_o^2)^2)^{1/2}$$

## References

1. G. M. Sheldrick, *Acta Crystallogr. A*, 2008, **64**, 112-122.
2. G. M. Sheldrick, *Acta Crystallogr. C Struct. Chem.*, 2015, **71**, 3-8.
3. O. V. Dolomanov, L. J. Bourhis, R. J. Gildea, J. A. K. Howard and H. Puschmann, *J. Appl. Crystallogr.* , 2009, **42**, 339-341.
4. A. L. Spek, *Acta Crystallogr., Sect D Biol. Crystallogr.*, 2009, **65**, 148-155.
5. J. He, J. Huang, Y. He, P. Cao, M. Zeller, A. D. Hunter and Z. Xu, *Chem - Eur. J.*, 2016, **22**, 1597-1601.